

Achieving more human brain-like vision via human EEG representational alignment

Zitong Lu ^{1,*}, Yile Wang ², Julie D. Golomb¹

¹Department of Psychology, The Ohio State University

²Department of Neuroscience, The University of Texas at Dallas

*email: lu.2637@osu.edu

Abstract

Despite advancements in artificial intelligence, object recognition models still lag behind in emulating visual information processing in human brains. Recent studies have highlighted the potential of using neural data to mimic brain processing; however, these often rely on invasive neural recordings from non-human subjects, leaving a critical gap in understanding human visual perception. Addressing this gap, we present, for the first time, ‘Re(presentational)Al(ignment)net’, a vision model aligned with human brain activity based on non-invasive EEG, demonstrating a significantly higher similarity to human brain representations. Our innovative image-to-brain multi-layer encoding framework advances human neural alignment by optimizing multiple model layers and enabling the model to efficiently learn and mimic human brain’s visual representational patterns across object categories and different modalities. Our findings suggest that ReAlnet represents a breakthrough in bridging the gap between artificial and human vision, and paving the way for more brain-like artificial intelligence systems.

Key words: Object Recognition; Neural Alignment; Human Brain-Like Model

1 Introduction

While current vision models in artificial intelligence (AI) are advanced, they still fall short of capturing the full complexity and adaptability inherent in the human brain’s information processing. Deep convolutional neural networks (DCNNs) have reached a performance level in object recognition that rivals human capabilities [1], and many studies have identified representational similarities in the hierarchical structure between DCNNs and the ventral visual stream [2, 3, 4, 5, 6]. However, the current alignment between DCNNs and human neural representations, while promising, still presents significant opportunities for further exploration and enhancement. Enhancing the resemblance between visual models and the human brain has become a critical concern for both computer scientists and neuroscientists. From a computer vision perspective, brain-inspired models often exhibit higher robustness and generalization, crucial for realizing true brain-like intelligence; meanwhile, from a cognitive neuroscience perspective, models that more closely mirror brain representations can significantly aid in our exploration of the brain’s visual processing mechanisms.

Given these challenges and limitations, the pivotal question arises is **how we can leverage our understanding of the human brain to enhance current AI vision models**. Conventional approaches have limitations in emulating the complexity of the human brain’s visual information processing, even with increased model depth and layers [7]. This limitation has prompted the exploration of new methodologies. Researchers have attempted various strategies, including *altering the model’s architecture* (adding recurrent structures [8, 4, 9, 10, 11], dual-pathway models [12, 13, 14, 15, 16], topographic constraints [17, 18, 19, 20] or feedback pathways [21]) and *changing the training task* (using self-supervised training [22, 23] or 3D task models [24]). However, can we directly use human neural activity to align ANNs on object recognition and achieve more human brain-like vision models?

Several previous studies have begun to try to apply neural data to machine learning especially deep learning models. The earliest attempt was to apply human fMRI signals to amend the classification boundary of SVMs and CNNs to achieve better category classification performance [25]. Some more recent studies started to let the models learn neural representations. One common way is to add a similarity loss to increase the representational similarity between models and neural activity (neural recordings obtained from mouse V1, monkey V1 or IT) during the training [26, 27, 28, 29]. Another strategy from [30] is to add an additional task based on an encoding module to predict monkey V1 neural activity. Both similarity-based method and multi-task framework can achieve more brain-like representations and improve model robustness. However, these neural alignment studies have two key challenges: (a) *Dependence on animal instead of human neural activity*. This limits the direct applicability and relevance of findings to human visual processing, and it is harder to enable models to effectively learn the human brain’s representational patterns because human non-invasive recording data usually have significantly lower data quality than data from animal invasive recordings. (b) *Single brain region or single model layer alignment*. On the one hand, previous studies just aligned a single early or late layer in CNN and/or align the model with a certain brain region, V1 or IT. On the other hand, it remains unclear which specific brain region should align with which particular layer of the model, leading to potential misalignment and inaccuracies. Additionally, a recent study focused on video emotion recognition first applied a representational similarity-based method to align CNN with human fMRI activity [31]. However, it is noteworthy that they focused on 6-category emotion classification tasks, may fall short in the more complex and diverse domain of object recognition which has larger space and multitude of object categories. Therefore, our work addressed this by employing an additional encoding module that goes beyond mere similarity. This module predicts human neural activity and is trained to autonomously extract complex visual features, offering a more effective approach for aligning the model with human neural representations in object recognition.

To bridge the gap between AI vision and human vision, we propose a more human brain-like vision model, ReAlnet, effectively aligned with human brain representations obtained from EEG recordings, based on a novel and effective encoding-based multi-layer alignment framework. Our representational

alignment framework allows us to obtain personalized vision models by aligning with individual’s neural data. To the best of our knowledge, we are the first to directly align object recognition models using non-invasive neural data recorded from human brains, which opens new possibilities for enhancing brain-like representations in models based on human brain activity. Moreover, the human brain-aligned ReAlnet shows improved similarity to human brain representations across different modalities (both human EEG and fMRI) and human behaviors.

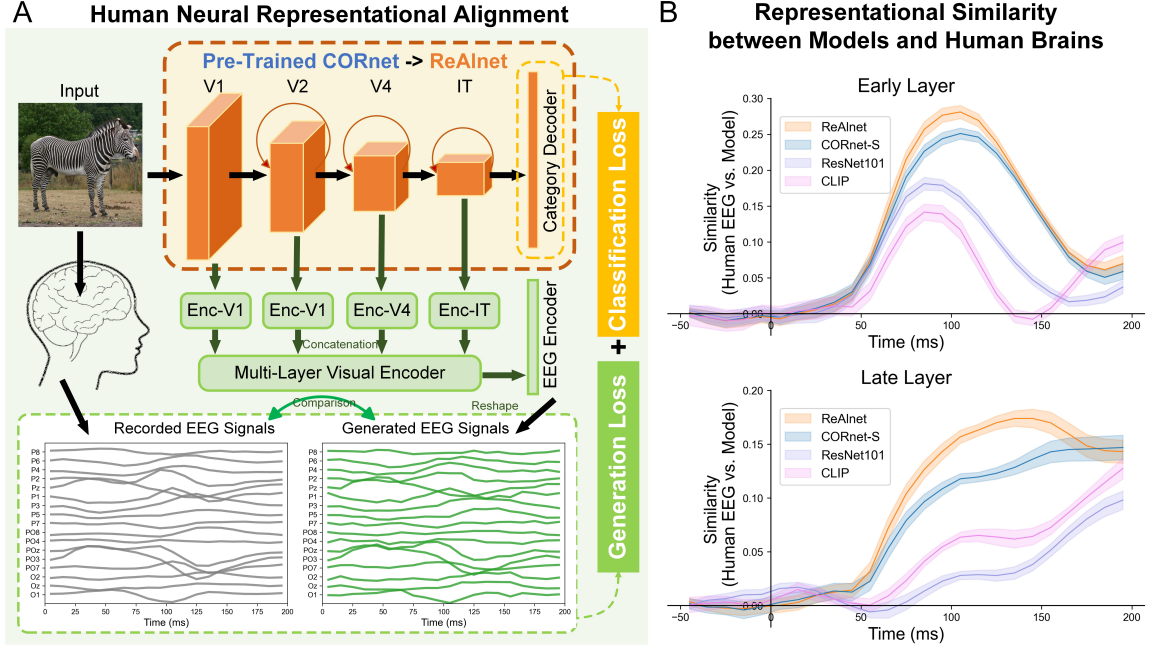


Figure 1: ReAlnet aligned with human EEG signals as a more human brain-like vision model. (A) An overview of ReAlnet alignment framework. Adding an additional multi-layer encoding module to an ImageNet pre-trained CORnet-S, the outputs contain the category classification results and the generated EEG signals. Using THINGS EEG2 training dataset, we aim to minimize both *classification loss* and *generation loss*, enabling CORnet to not only stabilize the classification performance but also effectively learn human brain features and transform into ReAlnet. (B) Using THINGS EEG2 test dataset, we measure the representational similarity between layer-wise internal representations in models and temporal EEG signals for early and late layers in ReAlnet, CORnet-S, ResNet101, and CLIP (with a ResNet101 backbone) respectively (early layer: the first layer; late layer: the layer before the classification layer in ReAlnet, CORnet, and ResNet, and the last visual layer in CLIP), and ReAlnet shows the highest similarity to the human brain.

2 Results

2.1 Aligning CORnet with human EEG representations

We applied a novel image-to-brain multiple-layer encoding alignment framework which let the model not only accurately classify the object category but also generate the realistic EEG signals via minimizing both classification and generation losses during the training (Figure 1A, see **Methods**). Based on this alignment framework, we build ten individual ReAlnets, using the state-of-the-art CORnet-S model [32, 9] as the foundational architecture. Each ReAlnet, which has the same architecture as CORnet, is additionally trained on a real human subject’s EEG signals, recorded while

viewing a massive number of natural images from THINGS EEG2 [33] training set. After training, We employed an independent test dataset consisting of 200 images and associated EEG activity from the THINGS EEG2 test set. These test set images had not been presented at all during the training process, coming from entirely novel (untrained) object categories. For models (ReAlnet and CORnet), we input these 200 images to each model and obtain the feature vectors corresponding to each image for each layer in the model. Then we calculated the temporal similarity between different models and human brain EEG based on the representational similarity analysis (RSA) method. Figure 1B shows the representational similarity between different models and temporal human brain EEG signals for early and late layers in ReAlnet, CORnet-S, ResNet101, and CLIP (with ResNet101 backbone) respectively, and ReAlnet aligned with human neural representations shows the highest similarity to the human brain.

In this study, our core focus is to investigate whether aligning the model with individual neural representations of humans can enhance the model’s similarity to the human brain. Our assessment of the models’ similarity to humans is not limited to its similarity with human brain EEG representations (based on THINGS EEG2 test set [33]); Similar to EEG, we then evaluated the model’s similarity to human brain fMRI representations (a completely different modality) from human subjects viewing novel image categories (based on Shen fMRI test set [34]). Additionally, we measured the similarity between the model and human behavior in several object recognition tasks using the Brain-Score platform [35] based on two behavioral benchmarks. For methodological details, refer to our Methods section. In the following sections, we elaborate on how ReAlnet – compared with the original CORnet not aligned with human neural data – more closely resembles human brain representations.

2.2 Improved similarity to human EEG

Here, for each of the 10 human subjects from the THINGS EEG2 dataset [33], we calculated (1) the similarity between their EEG data and CORnet (with the same structure as ReAlnet, but non aligned human neural data and non-individualized model), and (2) the similarity between their EEG data and the subject-matched ReAlnet via representational similarity analysis (RSA) based on THINGS EEG2 test dataset (See more details in Methods section). ReAlnets show significantly higher similarity to human EEG neural dynamics for all four visual layers (Layer V1: 70-130ms and 160-200ms; Layer V2: 60-200ms; Layer V4: 60-200ms; Layer IT: 70-160ms) than the original CORnet without human neural alignment (Figure 2A). Further statistical analysis of each layer’s similarity improvement (ReAlnet - CORnet) and improvement ratio $((\text{ReAlnet} - \text{CORnet}) / \text{CORnet})$ also indicate that at the similarity peak timepoint, there is a maximum of an 8% similarity improvement and an 80% improvement ratio, with the average improvement for the 50-200ms time-window being over 5% and the average improvement ratio over 40% (Figure 2B). It is worth noting that the test set doesn’t overlap with the training set in terms of object categories (concepts). Therefore, these significant improvements reveal ReAlnet’s generalization capability across different object categories.

These results suggest three findings: (1) Our multi-layer alignment framework indeed improves all layers’ similarity to human EEG representations. (2) Every ReAlnet with individual neural alignment exhibits improved similarity to human EEG compared to the basic CORnet. (3) Re-Alnets demonstrate the generalization of improvement in human brain-like similarity across object categories, as the image categories used for testing were entirely absent during the alignment training.

Additionally, unlike traditional models in computer vision, ReAlnet is a personalized model trained based on different individuals’ neural data. This sparked our interest in exploring whether these personalized ReAlnets exhibit intra-model individual variabilities and how such variabilities change across different layers of the model. To investigate this, we conducted comparisons between model RDMs based on 200 images in THINGS EEG2 test set across different layers, using the dissimilarity (one minus the Spearman correlation coefficient) between two RDMs corresponding to

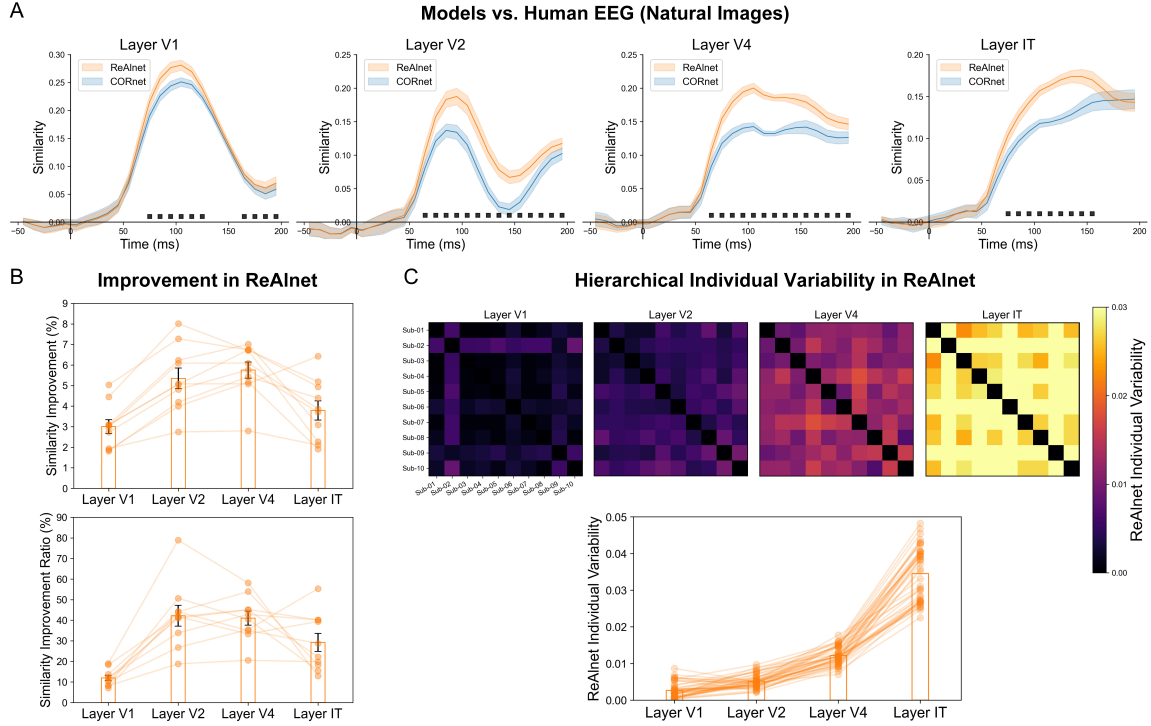


Figure 2: ReAlnets show higher similarity to human EEG and hierarchical individual variability. (A) Representational similarity time courses between human EEG and models (ReAlnet and CORnet) for different layers respectively. Black square dots at the bottom indicate the timepoints where ReAlnet vs. CORnet were significantly different ($p < .05$). Shaded area reflects \pm SEM. (B) Similarity improvement and similarity improvement ratio of ReAlnets compared to CORnet at the similarity peak timepoint. Each circle dot indicates an individual ReAlnet. (C) ReAlnet individual variability matrices of four visual layers and individual variability along layers. Each circle dot indicates a pair of two personalized ReAlnets.

two ReAlnets as an individual variability index. And our results show: (1) Personalized ReAlnets indeed exhibit individual variability (Figure 2C). (2) This variability increases with the depth of the layers (from Layer V1 to Layer IT, Figure 2C). This may also suggest a trend of increasing individual variability from primary to higher visual cortical areas in human brains.

2.3 Improved similarity in ReAlnets to human fMRI

Although ReAlnet demonstrates higher similarity to human EEG, a question arises: Does ReAlnet learn representations specific to EEG, or more general neural representations of the human brain? To ensure that our alignment framework enables the model to learn representations beyond the single modality of EEG, we utilized additional human fMRI data of three human subjects viewing natural images to evaluate the model’s cross-modality representational similarity to human fMRI.

Excitingly, we indeed observed an increase in this cross-modal brain-like similarity. Based on human fMRI signals of three subjects viewing 50 natural images, the similarity results indicate that even though ReAlnets were aligned based on human EEG data from different participants, they still resemble the human brain more closely on fMRI data compared to CORnet (Figure 3A). Also, there is a significant correlation of ReAlnets’ similarity improvement compared to CORnet between EEG and fMRI ($r = .9204, p < .001$) (Figure S1).

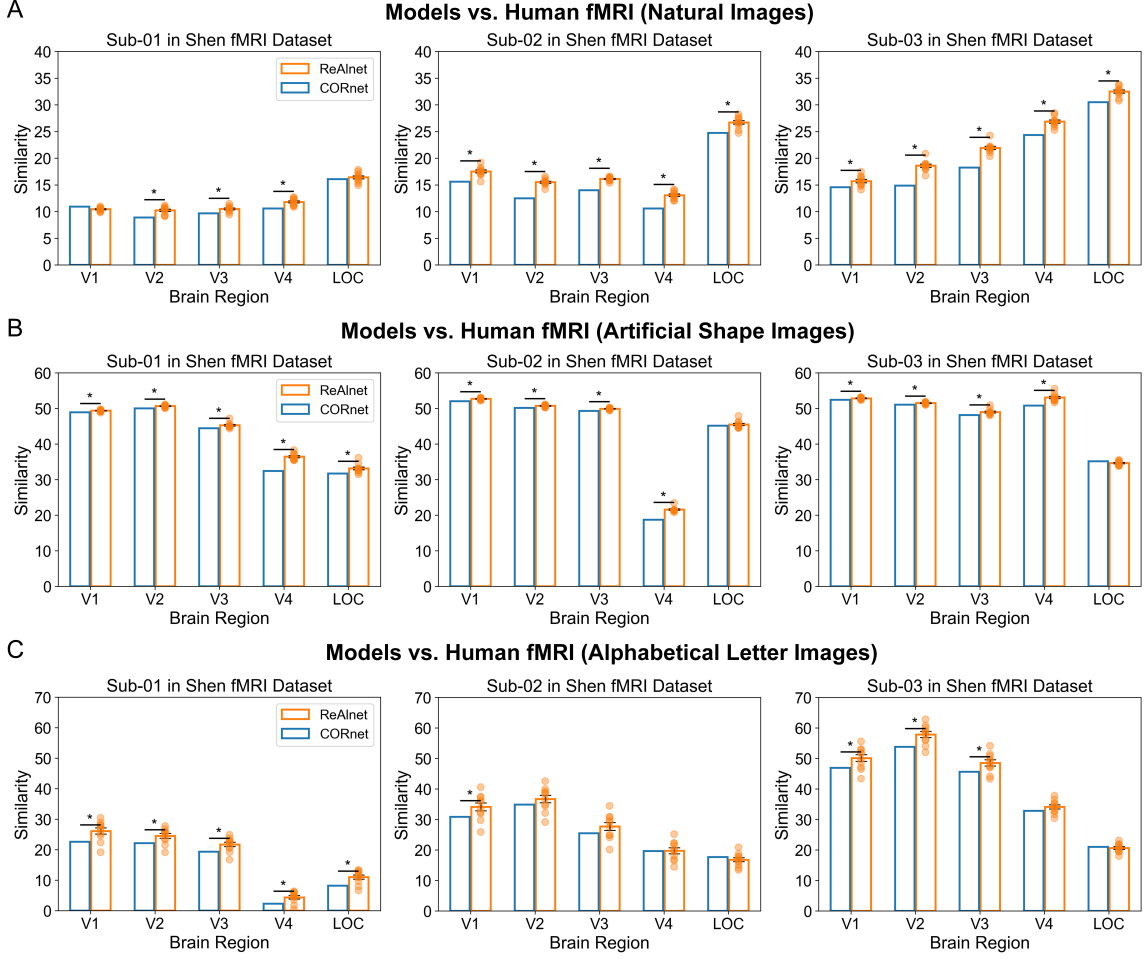


Figure 3: ReAlnets show higher similarity to human fMRI representations. Representational similarity between models and human fMRI of five different brain regions when three subjects viewed (A) natural images, (B) artificial shape images, and (C) alphabetical letter images. Asterisks indicate significantly higher similarity of ReAlnet than that of CORnet ($p < .05$). Each circle dot indicates an individual ReAlnet.

Additionally, to further assess the enhanced similarity between ReAlnet and human brain representations during image observation - not solely with natural images - we also measure the similarity between models and human fMRI signals from three subjects viewing 40 artificial shape and 10 alphabetical letter images in Shen fMRI test dataset. Although these images might be outside the natural image distribution, our results further demonstrate ReAlnet’s improved similarity to human brain representations in comparisons to CORnet (Figure 3B-C).

These findings further highlight three points: (1) Across multiple ROIs, ReAlnets exhibits higher human fMRI similarity than CORnet. (2) Despite not being trained with the EEG data of subjects in the fMRI dataset, almost every ReAlnet shows higher fMRI similarity, suggesting that ReAlnet learns consistent brain information processing patterns across subjects. (3) Images from fMRI dataset for evaluation were never presented during the alignment training, reaffirming the generalization of ReAlnets in improving brain-like similarity across object categories and images.

2.4 Improved similarity in ReAlnets to human behavior

Although the results above indicate that ReAlnet, which incorporates additional neural data alignment, demonstrates a higher similarity to human brain representations compared to CORnet, which is purely trained on images, it raises the question: does this neural-level alignment also translate into any behavioral alignment? To test whether ReAlnet shows improved similarity to human behavior, we calculated the scores of CORnet and 10 personalized ReAlnets based on the human behavioral assessments, including two object recognition tasks, in the Brain-Score platform. One task compared how well the ANN, compared to primates, could recognize objects presented in the center of their visual field, even when the objects varied in position, size, viewing angle, and background [7]. The other paradigm tested the similarity of behavioral error between the errors made by humans and ANN on an image-by-image basis [36]. These scores serve as indicators of the models’ similarity to human behavior. The average of two behavioral scores were used to compare with CORnet. Excitingly, the result reveals that ReAlnet, aligned with human EEG data, exhibits representations significantly more akin to human behavior than CORnet does ($t = 2.7702, p = .0217$), further expanding and emphasizing ReAlnet’s status as a more human brain-like vision model.

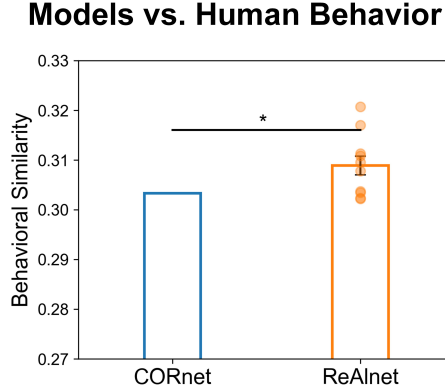


Figure 4: ReAlnets show higher similarity to human behavior based on the Brain-Score platform. Each circle dot indicates an individual ReAlnet. Asterisks indicate significantly higher similarity of ReAlnet than that of CORnet ($p < .05$).

2.5 Control experiments

For the control experiments, we tested two aspects: (1) How does contrastive learning influence model-to-brain alignment? (2) If we disrupt the pairing of each image with the EEG signal from the same subject but elicited by viewing a different image, can the model still learn the neural representation patterns of the human brain? Accordingly, we trained two additional sets of ReAlnets based on human EEG data from ten subjects in THINGS EEG2 dataset, termed as *W/o ContLoss* models (without the constrastive loss component) and Unpaired models (where the pairing between images and EEG signals was disrupted).

We tested the control models on the THINGS EEG2 test dataset and the Shen fMRI dataset, and calculated the similarity improvement for each control model compared to CORnet. Figure 5 plots the improvement in similarity (compared to CORnet baseline) for ReAlnet and the two controls. Here, we averaged the EEG similarity improvement of all layers and timepoints between 50 and 200ms, and averaged the fMRI similarity improvement of three subjects and five brain regions (See more detailed EEG and fMRI similarity results in Figure S2). The Unpaired control model showed no significant similarity improvement over CORnet for both EEG and fMRI modalities. The W/o ContLoss control model was significantly improved over CORnet for both modalities. W/o

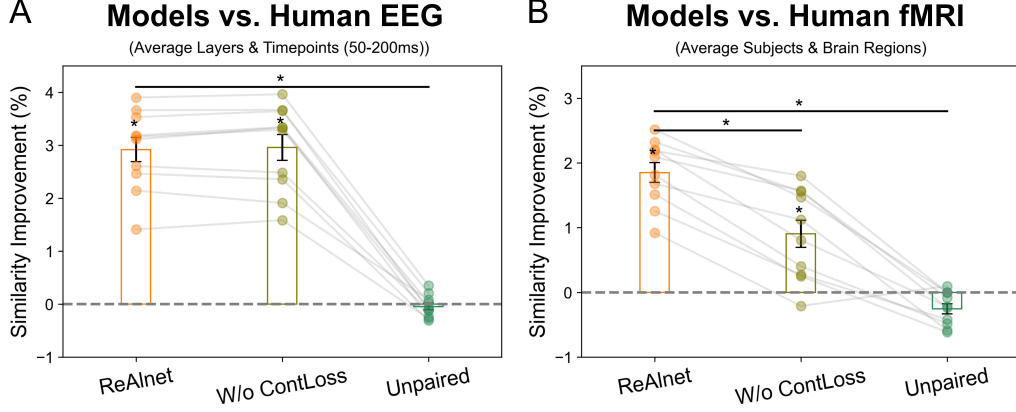


Figure 5: Results of control experiments. (A) Improvement in human EEG similarity of ReAlnets and control models compared to CORnet. (B) Improvement in human fMRI similarity of ReAlnets and control models compared to CORnet. Each circle dot indicates an individual model. Asterisks indicate the significance ($p < .05$).

ContLoss didn't perform as well as ReAlnet in terms of fMRI similarity ($t = -8.0353, p < .0001$) but showed similar improvement for EEG similarity ($t = .8543, p = .4151$). The results of the control experiments reveal (Figure 5A-B): (1) *W/o ContLoss* models still exhibit an improvement in human brain similarity compared to CORnet. However, while the similarity to human EEG did not decrease compared to ReAlnet, the similarity to cross-modality human fMRI significantly decreased. This suggests that the contrastive loss component in our alignment framework aids ReAlnet in extracting more cross-modality brain visual representation features. (2) Unpaired models failed to enhance brain similarity, which show no significant improvement in brain similarity compared to CORnet, indicating that the training process requires the model to effectively learn the specific neural visual features corresponding to each image. Only in this way can the model become more human brain-like and then exhibit higher similarity to the human brain across different object images, categories, and human neuroimaging data modalities.

2.6 Human EEG-aligned ResNet also being more brain-like

Although we trained ReAlnet based on CORnet and confirmed that it is more human brain-like, we also wondered whether our multi-layer encoding-based alignment framework could be extended to other models. Therefore, we chose ResNet18, a relatively larger model and aligned it with the EEG representations of ten subjects from THINGS EEG2 dataset using the strategy similar to how we trained ReAlnet. We refer to the aligned model based on pretrained ResNet18 as ReAlnet-R. Subsequently, we tested ReAlnet-Rs for their similarity to human EEG, fMRI, and behavior, comparing the results with those of the purely image-trained ResNet18.

Firstly, ReAlnet-Rs show significantly higher similarity to human EEG neural dynamics compared to ResNet for nearly all visual layers (Layer 1: 70-160ms, Layer 5: 60-200ms, Layer 9: 60-200ms, Layer 13: 60-180ms, Layer 17: 70-160ms, Figure 6A; See all layers' EEG similarity results in Figure S3). Secondly, personalized ReAlnet-Rs, similar to ReAlnet, exhibit individual variability increasing with the depth of the layers (Figure 6B; See all layers' individual variability matrices in Figure S4). Thirdly, ReAlnet-Rs also show higher similarity to human fMRI representations across multiple visual ROIs and different image categories (Figure 6C; See fMRI similarity results on all three subjects in Shen fMRI dataset in Figure S5). Fourthly, for human behavioral similarity, although it is not significant ($t = 1.6529, p = .1328$), seven out of ten ReAlnet-Rs show higher simi-

larity than original ResNet. These results collectively indicate that our alignment framework can be successfully extended to other visual models, such as ResNet, with ReAlnet-R still demonstrating improved similarity to human neural and behavioral representations.

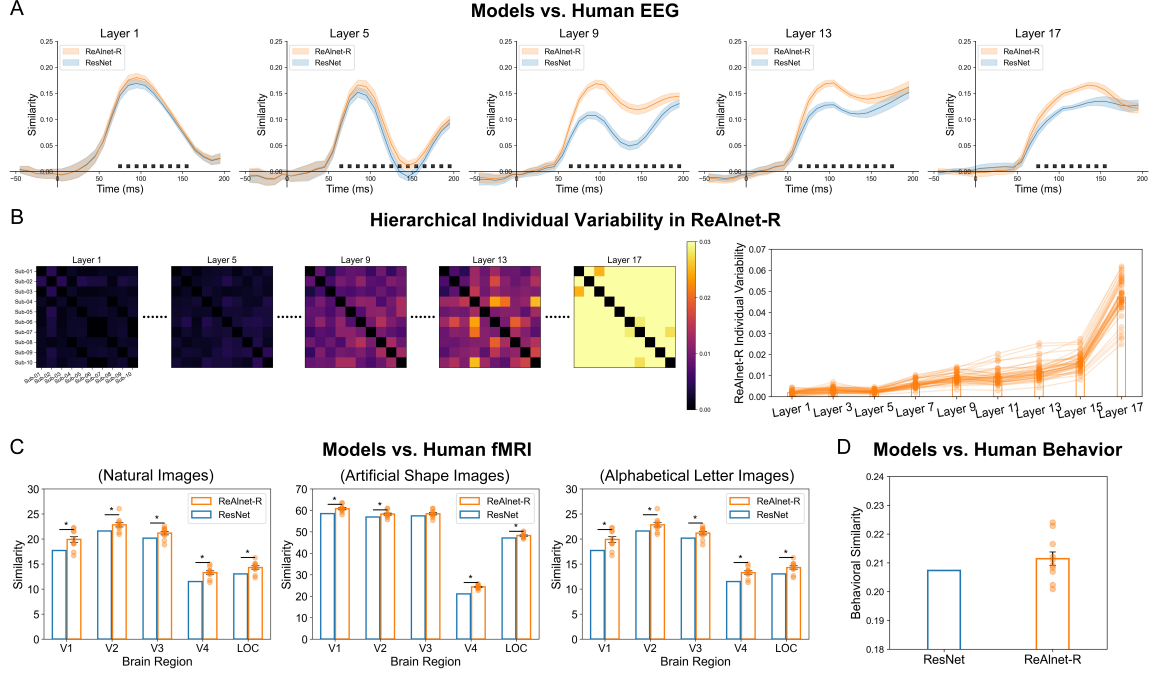


Figure 6: Similar improvements in ReAlnet-R. (A) Representational similarity time courses between human EEG and models (ReAlnet-R and ResNet) for layer 1, 5, 9, 13, and 17 respectively. Black square dots at the bottom indicate the timepoints where ReAlnet-R vs. ResNet were significantly different ($p < .05$). Shaded area reflects \pm SEM. (B) ReAlnet-R individual variability matrices of layer 1, 5, 9, 13, and 17 and individual variability along layers. Each circle dot indicates a pair of two personalized ReAlnets. (C) Representational similarity between models and human fMRI of five different brain regions when Subject 2 in Shen fMRI test dataset viewed natural, artificial shape, and alphabetical letter images. Asterisks indicate significantly higher similarity of ReAlnet-R than that of ResNet ($p < .05$). Each circle dot indicates an individual ReAlnet-R. (D) Similarity between models and human behavior based on the Brain-Score platform. Each circle dot indicates an individual ReAlnet-R.

3 Discussion

Building upon previous research utilizing neural data for aligning object recognition models, we propose a novel and more effective framework for human neural representational alignment, along with the corresponding human brain-like model, ReAlnet. Unlike previous studies that focused on using animal neural signals to optimize models or were unable to use global neural activity for comprehensive model optimization [26, 27, 28, 29, 30], our approach efficiently utilizes human neural activity to simultaneously optimize multiple layers of the model, enabling it to learn the human brain’s internal representational patterns for object visual processing. Notably, unlike prior research relying on behavioral or single modality neural recording data for model evaluation [26, 27, 31, 28, 29, 30], we employed different modalities of human neuroimaging data and also human behaviors for model evaluation to ensure that ReAlnet learns broader, cross-modal brain representational patterns. Additionally, we have extended our alignment framework to another convolutional neural network model to obtain ReAlnet-R and observed a similar enhancement in the similarity to human brain representations.

Regarding ReAlnet itself, it effectively learns not just the patterns of EEG data, but the brain’s internal processing patterns of visual information. This leads to ReAlnet exhibiting a higher similarity than the original CORnet not only to within-modality EEG but also to cross-modality fMRI and behavior. Recent studies in cognitive and computational neuroscience using the THINGS EEG2 dataset have traced evidence of human visual feature processing, including object categories, size, depth, image entropy [37, 38], and even reconstructing visual information through EEG signals [39, 40, 41] and realizing inter-subject EEG conversions [6]. These findings suggest that human brain EEG signals may contain more information than traditional convolutional neural networks can learn from images alone. Similar to this perspective, the fact that different generation loss weights do not significantly impact the model category classification performance but do enhance its similarity to human brains suggests that nodes in the model, which originally did not encode category-specific information, may have been optimized [27]. However, it does warrant further exploration to ascertain what specific information has been learned from the alignment with human brains. More analyses of the neural network’s internal representations may be needed to delve into this. Also, from a reverse-engineering perspective, attempting to understand the brain-like optimization process of the model could further aid in unraveling the mechanisms by which our brains process visual information [42, 43, 44, 45, 46].

Additionally, when we applied this alignment framework to ResNet18, the resulting ReAlnet-R still demonstrates more human brain-like representations, akin to those exhibited by ReAlnet. This framework’s generalizability may suggest that ReAlnet transcends being merely a specific vision model; it represents a pioneering framework potentially applicable for aligning other AI models with brain activity. Therefore, it is worth testing the generalization in the future. On the one hand, this alignment framework may be extended to other neural modalities, such as fMRI and MEG (dimensionality reduction might be necessary for extensive neural data features), paving the way for the development of variants like ReAlnet-fMRI and ReAlnet-MEG. On the other hand, another ambition is to adapt this framework to a wider range of models and tasks in the future, including language and auditory processing and self-supervised or unsupervised models, leading to innovations such as ReAlnet-Language, ReAlnet-Auditory, and self-supervised or unsupervised versions of ReAlnet.

Overall, our study transcends traditional boundaries by employing a groundbreaking alignment framework that pioneers the use of human neural data to achieve a more human brain-like vision model, ReAlnet. Demonstrating significant advances in bio-inspired AI, ReAlnet not only aligns closely with human EEG and fMRI but also exhibits hierarchical individual variabilities and increased similarity to human behavior, mirroring human visual processing. We hope that our alignment framework stands as a testament to the potential synergy between computational neuroscience and machine learning and enables the enhancement of any AI model to be more human brain-like, opening up exciting possibilities for future research in brain-like AI systems.

4 Methods

Here we describe the human neural data (EEG data for the alignment, and both EEG and fMRI data for testing the similarity between models and human brains) we used in this study, the alignment pipeline (including the structure, the loss functions, and training and test methods) for aligning the model representations with human neural representations, and the evaluation methods for measuring representational similarity between models and human brains and human behaviors.

4.1 Human EEG data for representational alignment

Human EEG data were obtained from an EEG open dataset, THINGS EEG2 [33], including EEG data from 10 healthy human subjects in a rapid serial visual presentation (RSVP) paradigm. Stimuli were images sized 500×500 pixels from THINGS dataset [47], which consists of images of objects on a natural background from 1854 different object concepts. Before inputting the images to the model, we reshaped image sizes to 224×224 pixels and normalized the pixel values of images to ImageNet statistics. Subjects viewed one image per trial (100ms). Each participant completed 66160 training set trials (1654 object concepts $\times 10$ images per concept $\times 4$ trials per image) and 16000 test set trials (200 object concepts $\times 1$ image per concept $\times 80$ trials).

EEG data were collected using a 64-channel EASYCAP and a BrainVision actiCHamp amplifier. We use already pre-processed data from 17 channels (O1, Oz, O2, PO7, PO3, POz, PO4, PO8, P7, P5, P3, P1, Pz, P2) overlying occipital and parietal cortex. We re-epoched EEG data ranging from stimulus onset to 200ms after onset with a sample frequency of 100Hz. Thus, the shape of our EEG data matrix for each trial is 17 channels \times 20 time points. and we reshaped the EEG data as a vector including 340 values for each trial. Before the model training and test, we averaged all the repeated trials (4 trials per image in the training set and 80 trials per image in the test set) to obtain more stable EEG signals.

It is worth noting that the training and test sets do not overlap in terms of object categories (concepts), which means that the performance of ReAlnet trained on the training set, when evaluated on the test set, can effectively reveal the model’s generalization capability across different object categories.

4.2 Human fMRI data for cross-modality testing

To demonstrate that our approach of aligning with human EEG not only enhances the model’s similarity to human EEG but indicates that ReAlnet has effectively learned the human brain’s representational patterns more broadly, we also performed cross-modal testing, testing ReAlnet on data from a different modality (fMRI), from a different set of subjects, viewing a different set of images. The fMRI data originate from [34]. This *Shen fMRI dataset* recorded human brain fMRI signals from three subjects while they focused on the center of the screen viewing images. We selected the test set from *Shen fMRI dataset*, which comprises fMRI signals of each subject viewing 50 natural images of different categories from ImageNet, 40 artificial shape images, and 10 alphabetical letter images with each image being viewed 24, 20, and 12 times respectively. We averaged the fMRI signals across the repeated trials to obtain more stable brain activity for each image observation and extracted signals from five regions-of-interest (ROIs) for subsequent comparison of model and human fMRI similarity: V1, V2, V3, V4, and the lateral occipital complex (LOC).

4.3 Image-to-brain encoding-based alignment pipeline

Basic architecture of ReAlnet and ReAlnet-R: We have chosen the state-of-the-art CORnet-S model [32, 9] as the foundational architecture for ReAlnet, incorporating recurrent connections akin to those in the biological visual system and proven to more closely emulate the brain’s visual processing. Both CORnet and ReAlnet consist of four visual layers (V1, V2, V4, and IT) and a category decoder layer. Layer V1 performs a 7×7 convolution with a stride of 2, followed by a 3×3 max pooling with a stride of 2, and another 3×3 convolution. Layer V2, V4, and IT each perform two 1×1 convolutions, a bottleneck-style 3×3 convolution with a stride of 2, and a 1×1 convolution. Apart from the initial Layer V1, the other three visual layers include recurrent connections, allowing outputs of a certain layer to be passed through the same layer several times (twice in Layer V2 and IT, and four times in Layer V4). We have also chosen another widely used model in image recognition, ResNet18, as the foundational architecture to obtain human EEG-aligned ReAlnet-R, which consists of 18 layers (the last layer is the final decoder to output the predicted category label).

EEG generation module: For ReAlnet, in addition to the original recurrent convolutional neural network structure, we have added an EEG generation module designed to construct an image-to-brain encoding model for generating realistic human EEG signals. Each visual layer is connected to a nonlinear $N \times 128$ layer-encoder (Enc-V1, Enc-V2, Enc-V4, and Enc-IT correspond to Layer V1, V2, V4, and IT) that processes through a fully connected network with a ReLU activation. These four layer-encoders are then directly concatenated to form an $N \times 512$ Multi-Layer Visual Encoder, which is subsequently connected to an $N \times 340$ EEG encoder through a linear layer to generate the predicted EEG signals. Here N is the batch size. For ReAlnet-R which is highly similar to ReAlnet, we extracted the features from Layer 5, Layer 9, Layer 13, and Layer 17 to connect to four nonlinear $N \times 128$ layer-encoders through fully connected networks with ReLU activations, and these four layer-encoders are then directly concatenated to form an $N \times 512$ Multi-Layer Visual Encoder, which is subsequently connected to an $N \times 340$ EEG encoder through a linear layer to generate the predicted EEG signals.

Therefore, we aim for the model to not only perform the object classification task but also to generate human EEG signals which can be highly similar to the real EEG signals when a person views the certain image through the EEG generation module with a series of encoders. During this process of generating brain activity, ReAlnet(-R)’s visual layers are poised to effectively extract features more aligned with neural representations.

Alignment Loss: Accordingly, the training loss \mathcal{L}^A of our alignment framework consists of two primary losses, a classification loss and a generation loss with a parameter β that determines the relative weighting:

$$\mathcal{L}^A = \mathcal{L}^C + \beta \cdot \mathcal{L}^G \quad (1)$$

\mathcal{L}^C represents the standard categorical cross entropy loss for model predictions on ImageNet labels:

$$\mathcal{L}^C = - \sum_{i=1}^N y_i \log(p_i) \quad (2)$$

Here, y_i represents the i -th image, and p_i represents the probability that model predicts the i -th image belongs to class i out of 1000 categories. However, the correct ImageNet category labels for images in THINGS dataset are not available. Therefore, we adopt the same strategy as in [26], using the labels obtained from the ImageNet pre-trained CORnet without neural alignment as the true

labels to stabilize the classification performance of ReAlnet.

\mathcal{L}^G is the generation loss, which includes a mean squared error (MSE) loss \mathcal{L}^{MSE} and a contrastive loss \mathcal{L}^{Cont} between the generated and real EEG signals. This contrastive loss is calculated based on the dissimilarity (1 minus Spearman correlation coefficient) between generated and real signals, aiming to bring the generated signals from the same image (positive pairs) closer to the corresponding real human EEG signals and make the generated signals from different images (negative pairs) more distinct. \mathcal{L}^G is calculated as followed:

$$\mathcal{L}^G = \mathcal{L}^{MSE} + \mathcal{L}^{Cont} \quad (3)$$

$$\mathcal{L}^{MSE} = \frac{1}{N} \sum_{i=1}^N (S_i - \hat{S}_i)^2 \quad (4)$$

$$\begin{aligned} \mathcal{L}^{Cont} = & \frac{1}{N} \sum_{i=1}^N [1 - \rho(S_i, \hat{S}_i)] \\ & - \frac{1}{N(N-1)} \sum_{i=1}^N \sum_{j=1, j \neq i}^N [1 - \rho(S_i, \hat{S}_j)] \end{aligned} \quad (5)$$

Here, S_i and \hat{S}_i represent the generated and real EEG signals corresponding to the i -th image.

Training procedures: Unlike CORnet and ResNet18 which trained on purely image-based ImageNet dataset, ReAlnet and ReAlnet-R additionally trained on individual EEG data. According to ten subjects in THINGS EEG2 dataset, we obtained ten personalized ReAlnets. Each network was trained to minimize the alignment loss including both classification and generation losses with a static loss weight β of 100 and a static training rate of 0.00002 for 30 epochs using the Adam optimizer. We used a batch size of 16, meaning the contrastive loss computed dissimilarities of 256 pairs for each gradient step.

Additionally, for ReAlnet, we applied other three different β weights ($\beta = 1, 10$, or 1000) separately to train the model to further explore the impact of this β value on the performance of ReAlnet. We observed that with an increase in β , ReAlnets show greater similarity to human EEG and fMRI and more pronounced individual variability within models. However, only ReAlnet with $\beta = 100$ show significantly higher similarity to human behaviors. Thus, we suggest that $\beta = 100$ could be the best parameter to conduct the human EEG alignment. Figures S6 to S10 show the performance and similarity results of ReAlnets with different β values.

We tested the classification accuracy of ReAlnets on ImageNet at different β values (Figure S6). Importantly, to ascertain that the observed decrease in accuracy was not due to the additional generation task compromising classification performance, but rather the absence of correct ImageNet labels for images in THINGS EEG2 dataset, we trained a ReAlnet with $\beta = 0$. This ReAlnet excluded the EEG signal generation module but underwent fine-tuning with images from THINGS EEG2 dataset. The results indicated that the ReAlnet with $\beta = 0$ also experienced a similar level of decline.

4.4 Model-human similarity measurement

Neural similarity via Representational similarity analysis (RSA): RSA is used for representational comparisons between models and human brains [48] based on first computing representational dissimilarity matrices (RDMs) for models and human neural signals, and then calculating Spearman correlation coefficients between RDMs from two systems.

To evaluate the similarity between models and human EEG, the shape of each RDM is 200×200 , corresponding to 200 images in THINGS EEG2 test set. For EEG RDMs, we applied decoding accuracy between two image conditions as the dissimilarity index to construct EEG RDM for each timepoint and each subject. For model RDMs, we input 200 images into each model and obtained latent features from each visual layer. Then, we constructed each layer’s RDM by calculating the dissimilarity using 1 minus Pearson correlation coefficient between flattened vectors of latent features corresponding to any two images. To compare the representations, we calculated the Spearman correlation coefficient as the similarity index between layer-by-layer model RDMs and timepoint-by-timepoint neural EEG RDMs.

To evaluate the similarity between models and human fMRI, the shape of each RDM (natural images, artificial shape images, or alphabetical letter images) is 50×50 , 40×40 , or 10×10 in Shen fMRI dataset test set. For fMRI RDMs, we calculated 1 minus Pearson correlation coefficient between voxel-wise activation patterns corresponding to any two images as the dissimilarity index in the RDM for each ROI and each subject. For model RDMs, similar to the EEG comparisons above, we obtained the RDM for each layer from each model. Then, we calculated the Spearman correlation coefficient as the similarity index between layer-by-layer model RDMs and neural fMRI RDMs for different ROIs, assigning the final similarity for a certain brain region as the highest similarity result across model layers due to the lack of a clear correspondence between different model layers and brain regions. All RSA analyses were implemented based on NeuroRA toolbox [49].

Behavioral similarity via Brain-Score:

Brain-Score is a framework that evaluates how similar artificial neural networks (ANNs) are to the primate visual system [35]. To measure the behavioral similarity between ReAlnet and humans (and monkeys) in visual recognition tasks, we used two behavioral benchmarks from the Brain-Score framework: (<https://github.com/brain-score/vision>). "Rajalingham2018public-i2n" assesses the ability of recognizing core objects from visual images, even with various changes in position, size, viewing angle, and background of the objects[7]. "Geirhos2021-error_consistency" measures the similarity of errors made by ANN and human. Here, metrics of error consistency were adopted in our study, which measure whether there is above-chance overlap in the specific images that humans and models classify incorrectly. [36]. The behavioral Brain-Score is calculated by taking the average of two behavioral benchmarks. We compared the results from ReAlnets and ReAlnet-Rs to the behavioral Brain-Score of CORnet and ResNet respectively, using the same benchmarks. For more detailed information about the behavioral benchmarks used in this study, please refer to the original papers by [35, 7, 36].

Acknowledgment

This work was supported by grants from the National Institutes of Health (R01-EY025648) and National Science Foundation (NSF 1848939) to Julie D. Golomb. We thank the Ohio Supercomputer Center and Georgia Stuart for providing the essential computing resources and support. We thank Yuxuan Zeng for the ‘ReAlnet’ name suggestion. We thank Tianyu Zhang, Shuai Chen, Jiaqi Li, and some other members in Memory & Perception Reviews Reading Group (RRG) for helpful discussions about the methods and results. We thank Yuxin Wang for constructive feedback on the manuscript.

References

- [1] Yann Lecun, Yoshua Bengio, and Geoffrey Hinton. Deep learning. *Nature*, 521(7553), 2015.

- [2] Radoslaw Martin Cichy, Aditya Khosla, Dimitrios Pantazis, Antonio Torralba, and Aude Oliva. Comparison of deep neural networks to spatio-temporal cortical dynamics of human visual object recognition reveals hierarchical correspondence. *Scientific Reports*, 6(1):1–13, 2016.
- [3] Umut Güçlü and Marcel A.J. van Gerven. Deep Neural Networks Reveal a Gradient in the Complexity of Neural Representations across the Ventral Stream. *Journal of Neuroscience*, 35(27):10005–10014, 2015.
- [4] Tim C. Kietzmann, Courtney J. Spoerer, Lynn K.A. Sörensen, Radoslaw M. Cichy, Olaf Hauk, and Nikolaus Kriegeskorte. Recurrence is required to capture the representational dynamics of the human visual system. *Proceedings of the National Academy of Sciences of the United States of America*, 116(43):21854–21863, 2019.
- [5] Daniel L.K. Yamins, Ha Hong, Charles F. Cadieu, Ethan A. Solomon, Darren Seibert, and James J. DiCarlo. Performance-optimized hierarchical models predict neural responses in higher visual cortex. *Proceedings of the National Academy of Sciences of the United States of America*, 111(23):8619–8624, 2014.
- [6] Zitong Lu and Julie D Golomb. Generate your neural signals from mine: individual-to-individual EEG converters. *Proceedings of the Annual Meeting of the Cognitive Science Society 45*, 2023.
- [7] Rishi Rajalingham, Elias B. Issa, Pouya Bashivan, Kohitij Kar, Kailyn Schmidt, and James J. DiCarlo. Large-Scale, High-Resolution Comparison of the Core Visual Object Recognition Behavior of Humans, Monkeys, and State-of-the-Art Deep Artificial Neural Networks. *Journal of Neuroscience*, 38(33):7255–7269, 2018.
- [8] Kohitij Kar, Jonas Kubilius, Kailyn Schmidt, Elias B. Issa, and James J. DiCarlo. Evidence that recurrent circuits are critical to the ventral stream’s execution of core object recognition behavior. *Nature Neuroscience*, 22(6):974–983, 2019.
- [9] Jonas Kubilius, Martin Schrimpf, Kohitij Kar, Rishi Rajalingham, Ha Hong, Najib J Majaaj, Elias B Issa, Pouya Bashivan, Jonathan Prescott-Roy, Kailyn Schmidt, Aran Nayebi, Daniel Bear, Daniel L K Yamins, and James J Dicarlo. Brain-Like Object Recognition with High-Performing Shallow Recurrent ANNs. *Advances in Neural Information Processing Systems (NeurIPS)*, 32, 2019.
- [10] Courtney J. Spoerer, Patrick McClure, and Nikolaus Kriegeskorte. Recurrent convolutional neural networks: A better model of biological object recognition. *Frontiers in Psychology*, 8:1551, 2017.
- [11] Hanlin Tang, Martin Schrimpf, William Lotter, Charlotte Moerman, Ana Paredes, Josue Ortega Caro, Walter Hardesty, David Cox, and Gabriel Kreiman. Recurrent computations for visual pattern completion. *Proceedings of the National Academy of Sciences of the United States of America*, 115(35):8835–8840, 2018.
- [12] Shuang Bai, Zhaohong Li, and Jianjun Hou. Learning two-pathway convolutional neural networks for categorizing scene images. *Multimedia Tools and Applications*, 76(15):16145–16162, 2017.
- [13] Minkyu Choi, Kuan Han, Xiaokai Wang, Yizhen Zhang, and Zhongming Liu. A Dual-Stream Neural Network Explains the Functional Segregation of Dorsal and Ventral Visual Pathways in Human Brains. *Advances in Neural Information Processing Systems (NeurIPS)*, 36, 2023.
- [14] Zhixian Han and Anne Sereno. Modeling the Ventral and Dorsal Cortical Visual Pathways Using Artificial Neural Networks. *Neural Computation*, 34(1):138–171, 2022.
- [15] Zhixian Han and Anne Sereno. Identifying and Localizing Multiple Objects Using Artificial Ventral and Dorsal Cortical Visual Pathways. *Neural Computation*, 35(2):249–275, 2023.
- [16] Tiancheng Sun, Yulong Wang, Jian Yang, and Xiaolin Hu. Convolution Neural Networks With Two Pathways for Image Style Recognition. *IEEE Transactions on Image Processing*, 26(9):4102–4113, 2017.

- [17] Dawn Finzi, Eshed Margalit, Kendrick Kay, Daniel L K Yamins, and Kalanit Grill-Spector. Topographic DCNNs trained on a single self-supervised task capture the functional organization of cortex into visual processing streams. *NeurIPS 2022 Workshop SVRHM*, 2022.
- [18] Hyodong Lee, Eshed Margalit, Kamila M. Jozwik, Michael A. Cohen, Nancy Kanwisher, Daniel L. K. Yamins, and James J. DiCarlo. Topographic deep artificial neural networks reproduce the hallmarks of the primate inferior temporal cortex face processing network. *bioRxiv*, 2020.
- [19] Zejin Lu, Adrien Doerig, Victoria Bosch, Bas Krahmer, Daniel Kaiser, Radoslaw M Cichy, and Tim C Kietzmann. End-to-end topographic networks as models of cortical map formation and human visual behaviour: moving beyond convolutions. *arXiv*, 2023.
- [20] Eshed Margalit, Hyodong Lee, Dawn Finzi, James J. DiCarlo, Kalanit Grill-Spector, and Daniel L.K. Yamins. A Unifying Principle for the Functional Organization of Visual Cortex. *bioRxiv*, 2023.
- [21] Talia Konkle and George Alvarez. Cognitive Steering in Deep Neural Networks via Long-Range Modulatory Feedback Connections. *Advances in Neural Information Processing Systems (NeurIPS)*, 2023.
- [22] Talia Konkle and George A. Alvarez. A self-supervised domain-general learning framework for human ventral stream representation. *Nature Communications*, 13(1):1–12, 2022.
- [23] Jacob S. Prince, George A. Alvarez, and Talia Konkle. A contrastive coding account of category selectivity in the ventral visual stream. *bioRxiv*, 2023.
- [24] Thomas P. O’Connell, Tyler Bonnen, Yoni Friedman, Ayush Tewari, Josh B. Tenenbaum, Vincent Sitzmann, and Nancy Kanwisher. Approaching human 3D shape perception with neurally mappable models. *arXiv*, 2023.
- [25] Ruth C. Fong, Walter J. Scheirer, and David D. Cox. Using human brain activity to guide machine learning. *Scientific Reports*, 8(1):1–10, 2018.
- [26] Joel Dapello, Kohitij Kar, Martin Schrimpf, Robert Baldwin Geary, Michael Ferguson, David Daniel Cox, and James J. DiCarlo. Aligning Model and Macaque Inferior Temporal Cortex Representations Improves Model-to-Human Behavioral Alignment and Adversarial Robustness. *International Conference on Learning Representations (ICLR)*, 12, 2023.
- [27] Callie Federer, Haoyan Xu, Alona Fyshe, and Joel Zylberberg. Improved object recognition using neural networks trained to mimic the brain’s statistical properties. *Neural Networks*, 131:103–114, 2020.
- [28] Zhe Li, Wieland Brendel, Edgar Y. Walker, Erick Cobos, Taliah Muhammad, Jacob Reimer, Matthias Bethge, Fabian H. Sinz, Xaq Pitkow, and Andreas S. Tolias. Learning from brains how to regularize machines. *Advances in Neural Information Processing Systems (NeurIPS)*, 32, 2019.
- [29] Cassidy Pirlot, Richard C. Gerum, Cory Efird, Joel Zylberberg, and Alona Fyshe. Improving the Accuracy and Robustness of CNNs Using a Deep CCA Neural Data Regularizer. *arXiv*, 2022.
- [30] Shahd Safarani, Arne Nix, Konstantin Willeke, Santiago A. Cadena, Kelli Restivo, George Denfield, Andreas S. Tolias, and Fabian H. Sinz. Towards robust vision by multi-task learning on monkey visual cortex. *Advances in Neural Information Processing Systems (NeurIPS)*, 34, 2021.
- [31] Kaicheng Fu, Changde Du, Shengpei Wang, and Huiguang He. Improved Video Emotion Recognition with Alignment of CNN and Human Brain Representations. *IEEE Transactions on Affective Computing*, 14(8):1–15, 2023.
- [32] J. Kubilius, M. Schrimpf, A. Nayeibi, D. Bear, D.L.K. Yamins, and J.J. DiCarlo. CORnet: Modeling the Neural Mechanisms of Core Object Recognition. *bioRxiv*, 2018.

- [33] Alessandro T. Gifford, Kshitij Dwivedi, Gemma Roig, and Radoslaw M. Cichy. A large and rich EEG dataset for modeling human visual object recognition. *NeuroImage*, 264:119754, 2022.
- [34] Guohua Shen, Tomoyasu Horikawa, Kei Majima, and Yukiyasu Kamitani. Deep image reconstruction from human brain activity. *PLoS computational biology*, 15(1):e1006633, 2019.
- [35] Martin Schrimpf, Jonas Kubilius, Ha Hong, Najib J. Maja, Rishi Rajalingham, Elias B. Issa, Kohitij Kar, Pouya Bashivan, Jonathan Prescott-Roy, Franziska Geiger, Kailyn Schmidt, Daniel L. K. Yamins, and James J. DiCarlo. Brain-Score: Which Artificial Neural Network for Object Recognition is most Brain-Like? *bioRxiv*, 2020.
- [36] Robert Geirhos, Kantharaju Narayanappa, Benjamin Mitzkus, Tizian Thieringer, Matthias Bethge, Felix A Wichmann, and Wieland Brendel. Partial success in closing the gap between human and machine vision. *NeurIPS*, 2021.
- [37] Zitong Lu and Julie D Golomb. Human EEG and artificial neural networks reveal disentangled representations of object real-world size in natural images. *bioRxiv*, 2023.
- [38] I. Muukkonen and V.R. Salmela. Entropy predicts early MEG, EEG and fMRI responses to natural images. *bioRxiv*, 2023.
- [39] Dongyang Li, Chen Wei, Shiyang Li, Jiachen Zou, and Quanying Liu. Visual Decoding and Reconstruction via EEG Embeddings with Guided Diffusion. *arXiv*, 2024.
- [40] Changde Du, Kaicheng Fu, Jinpeng Li, and Huiguang He. Decoding Visual Neural Representations by Multimodal Learning of Brain-Visual-Linguistic Features. *IEEE Transactions on Pattern Analysis and Machine Intelligence*, 45(9):10760–10777, 2023.
- [41] Yonghao Song, Bingchuan Liu, Xiang Li, Nanlin Shi, Yijun Wang, and Xiaorong Gao. Decoding Natural Images from EEG for Object Recognition. *arXiv*, 2023.
- [42] Vladislav Ayzenberg, Nicholas Blauch, and Marlene Behrmann. Using deep neural networks to address the how of object recognition. *PsyArXiv*, 2023.
- [43] Radoslaw M. Cichy and Daniel Kaiser. Deep Neural Networks as Scientific Models. *Trends in Cognitive Sciences*, 23(4):305–317, 2019.
- [44] Adrien Doerig, Rowan Sommers, Katja Seeliger, Blake Richards, Jenann Ismael, Grace Lindsay, Konrad Kording, Talia Konkle, Marcel A. J. Van Gerven, Nikolaus Kriegeskorte, and Tim C. Kietzmann. The neuroconnectionist research programme. *Nature Reviews Neuroscience*, 24:431–450, 2023.
- [45] Nancy Kanwisher, Meenakshi Khosla, and Katharina Dobs. Using artificial neural networks to ask ‘why’ questions of minds and brains. *Trends in Neurosciences*, 46(3):240–254, 2023.
- [46] Zitong Lu and Yixuan Ku. Bridging the gap between EEG and DCNNs reveals a fatigue mechanism of facial repetition suppression. *iScience*, 26:108501, 2023.
- [47] Martin N. Hebart, Adam H. Dickter, Alexis Kidder, Wan Y. Kwok, Anna Corriveau, Caitlin Van Wicklin, and Chris I. Baker. THINGS: A database of 1,854 object concepts and more than 26,000 naturalistic object images. *PLoS ONE*, 14(10):1–24, 2019.
- [48] Nikolaus Kriegeskorte, Marieke Mur, and Peter Bandettini. Representational similarity analysis - connecting the branches of systems neuroscience. *Frontiers in Systems Neuroscience*, 4, 2008.
- [49] Zitong Lu and Yixuan Ku. NeuroRA: A Python Toolbox of Representational Analysis From Multi-Modal Neural Data. *Frontiers in Neuroinformatics*, 14:61, 2020.

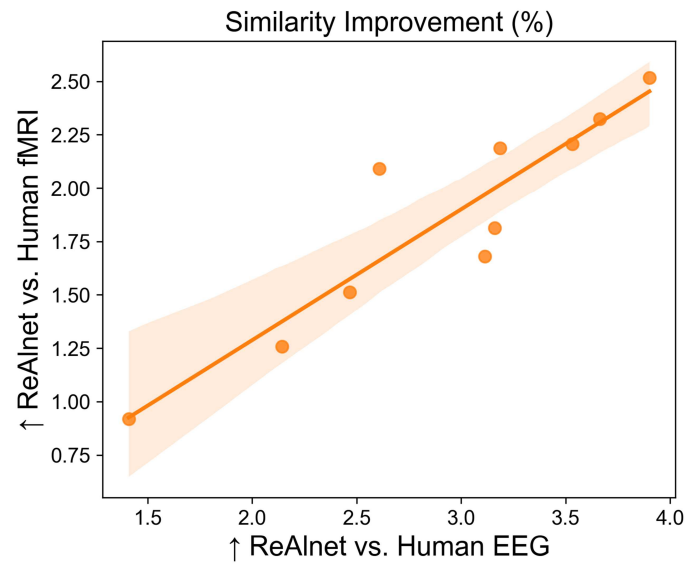


Figure S1: Correlation of similarity improvement between ReAlnet vs. human EEG and ReAlnet vs. human fMRI. Each circle dot indicates an individual ReAlnet.

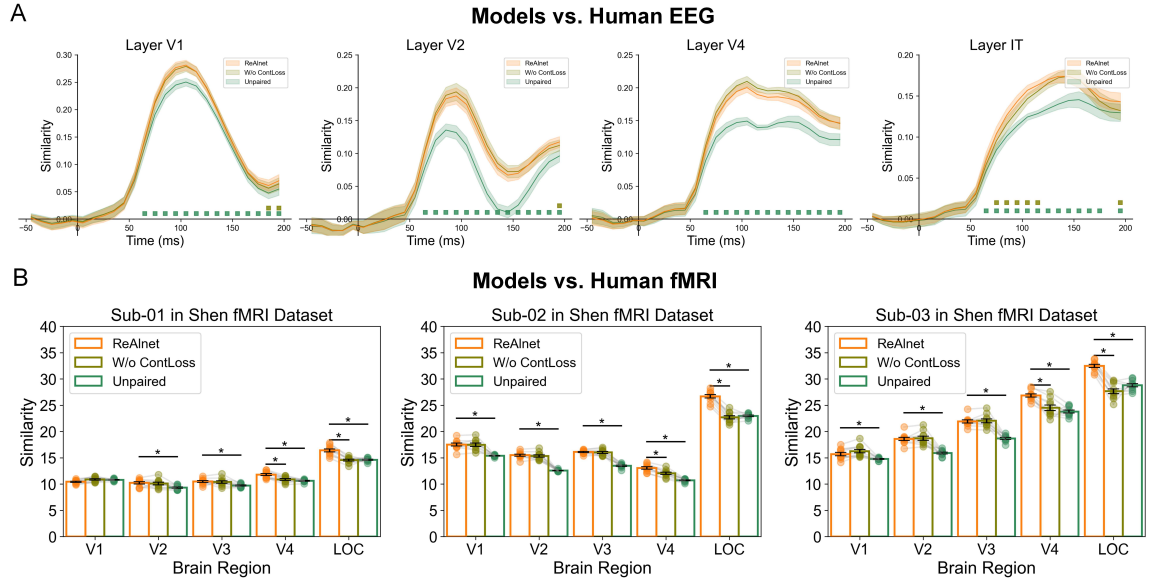


Figure S2: (A) Representational similarity time courses between human EEG and ReAlnets and control models ($\beta = 100$) for different layers respectively. Shaded area reflects \pm SEM. Olive and seagreen square dots at the bottom indicate the timepoints where ReAlnet was significantly higher than W/o ContLoss and Unpaired models respectively ($p < .05$). (B) Representational similarity between three subjects' fMRI activity of five different brain regions and ReAlnets and control models ($\beta = 100$) respectively. Asterisks indicate significantly higher similarity of ReAlnet than that of control models ($p < .05$).

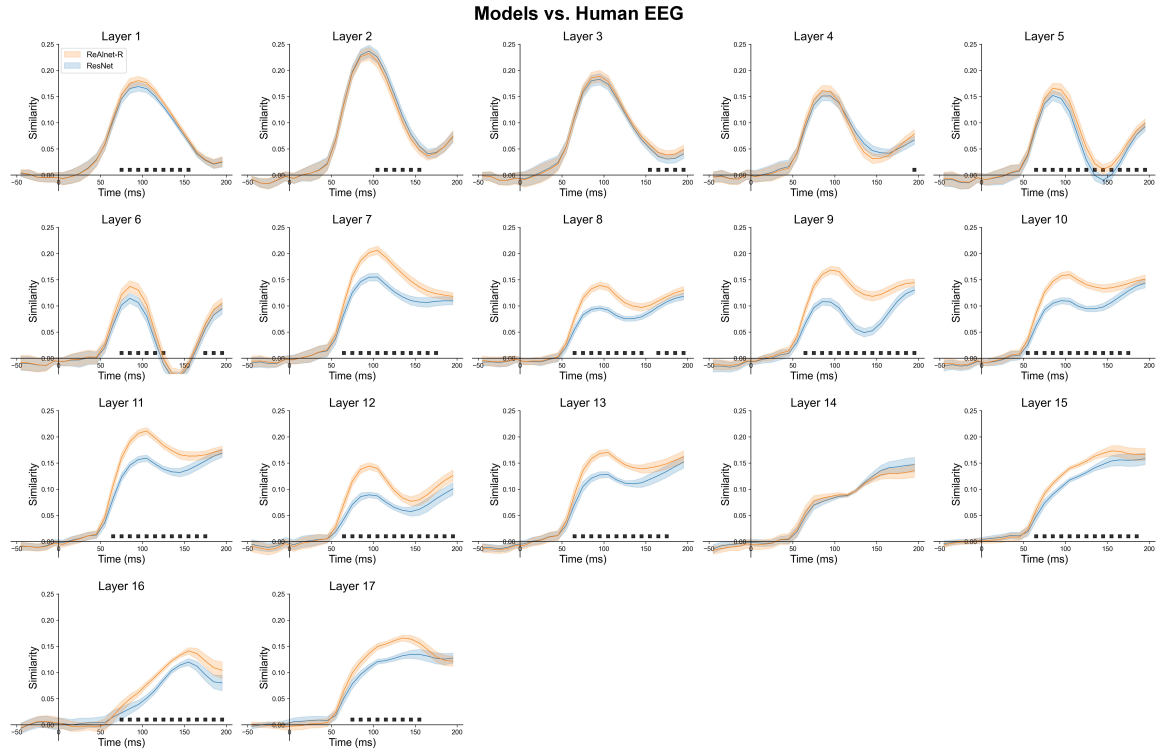


Figure S3: Representational similarity time courses between human EEG and models (ReAlnet-R and ResNet) for all 17 layers respectively. Black square dots at the bottom indicate the timepoints where ReAlnet-R was significantly higher than ResNet ($p < .05$). Shaded area reflects \pm SEM.

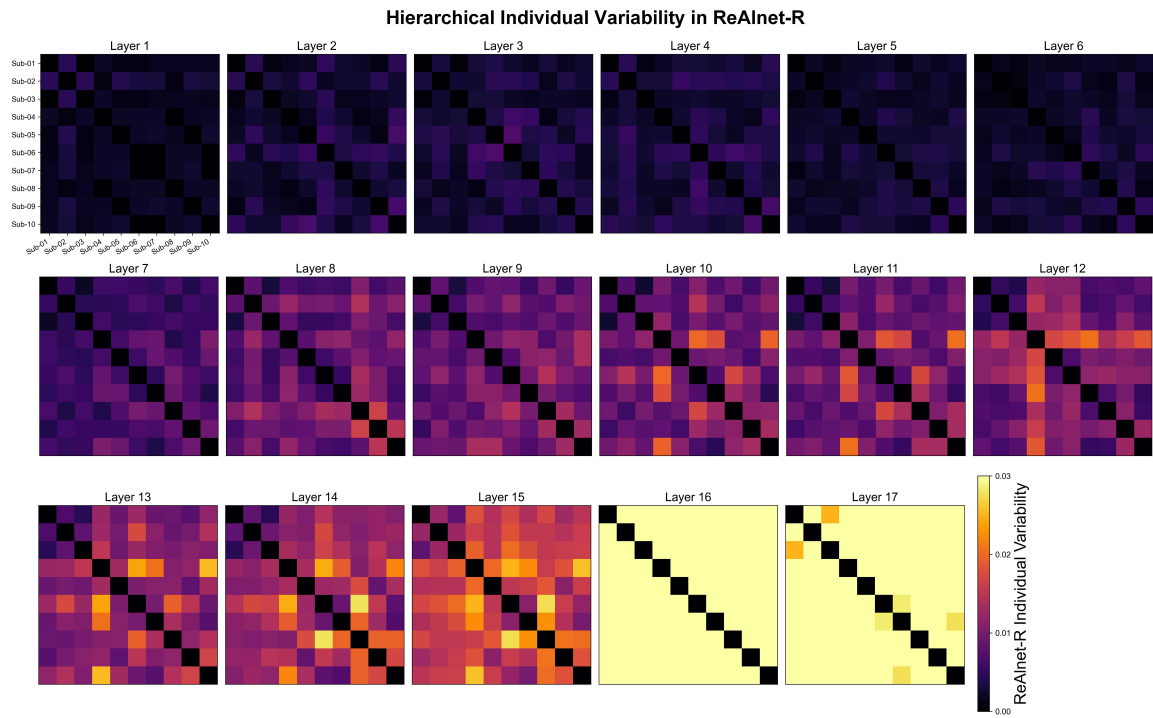


Figure S4: ReAlnet-R individual variability matrices of all layers. Each circle dot indicates a pair of two personalized ReAlnet-Rs.

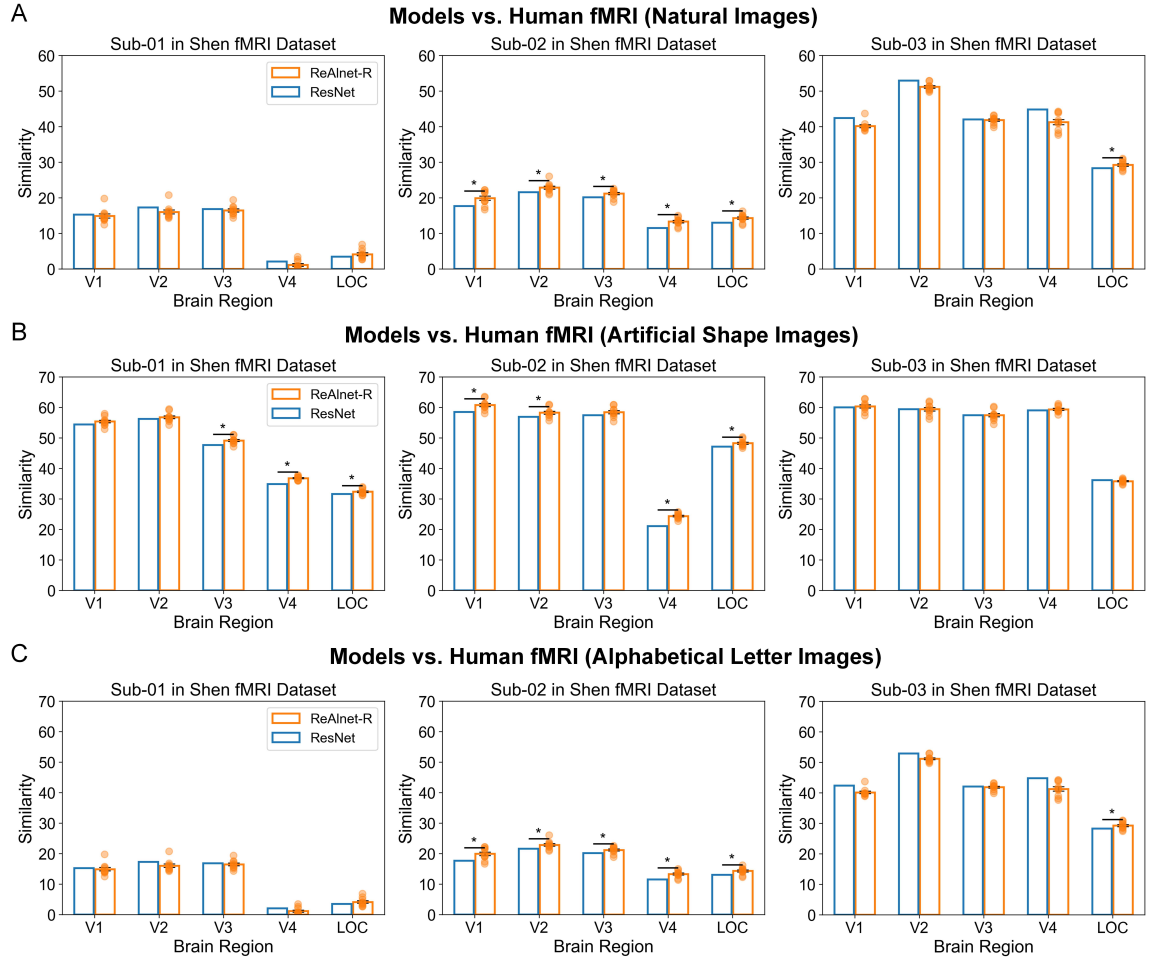


Figure S5: Representational similarity between models and human fMRI of five different brain regions when three subjects viewed (A) natural images, (B) artificial shape images, and (C) alphabetical letter images. Asterisks indicate significantly higher similarity of ReAlnet-R than that of Resnet ($p < .05$). Each circle dot indicates an individual ReAlnet-R.

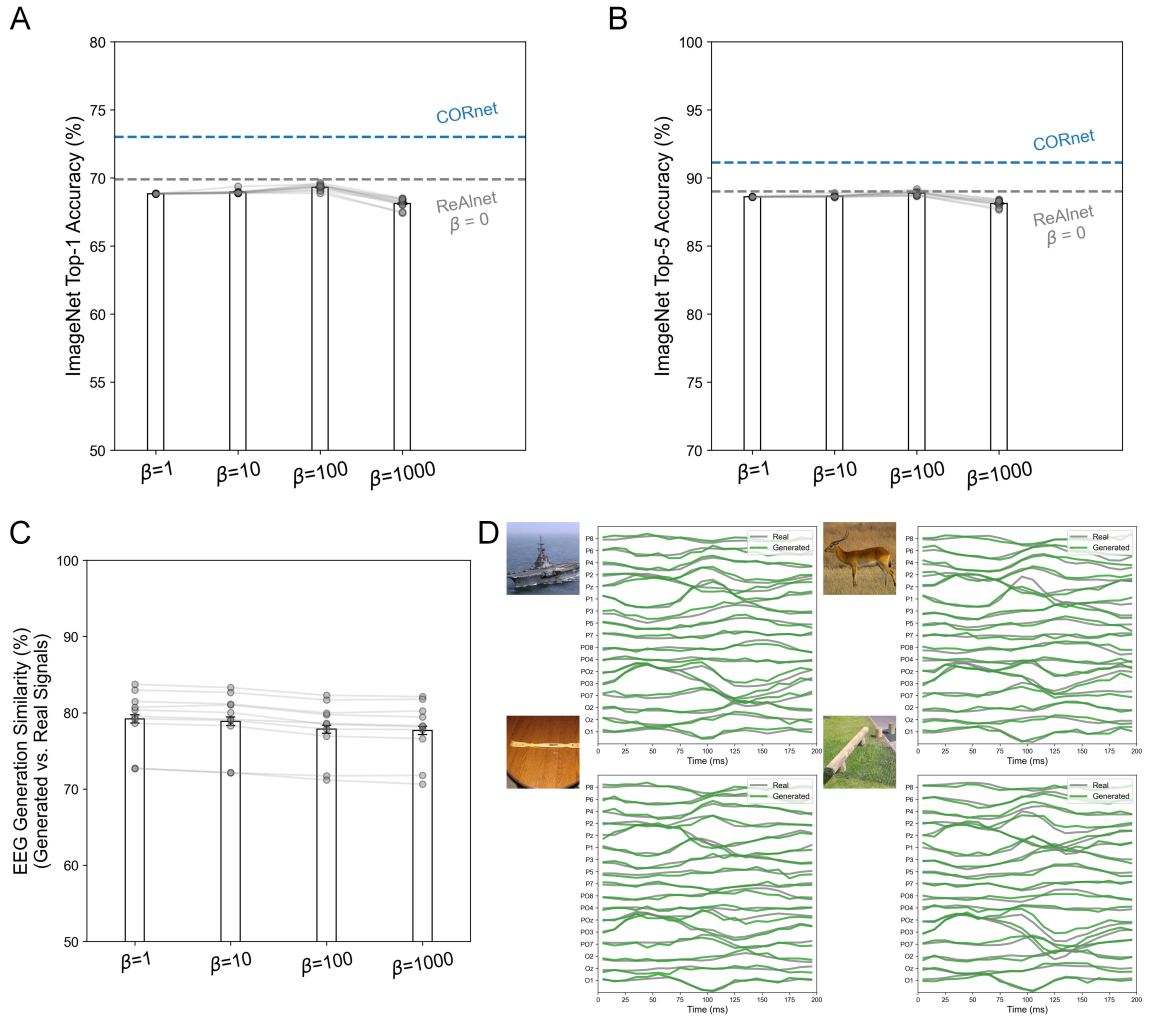


Figure S6: ReAlnets' object category classification and EEG generation performances. (A) Top-1 and (B) Top-5 ImageNet classification accuracy of different ReAlnets. (C) EEG generation performance of different ReAlnets. (D) Four examples of EEG generation results (from the model at $\beta = 100$ of Sub-01). For each example, the left image indicates the image input to the ReAlnet and the image viewed by the subject. The grey curves represent the real EEG signals, and the green curves represent the generated EEG signals corresponding to the same image.

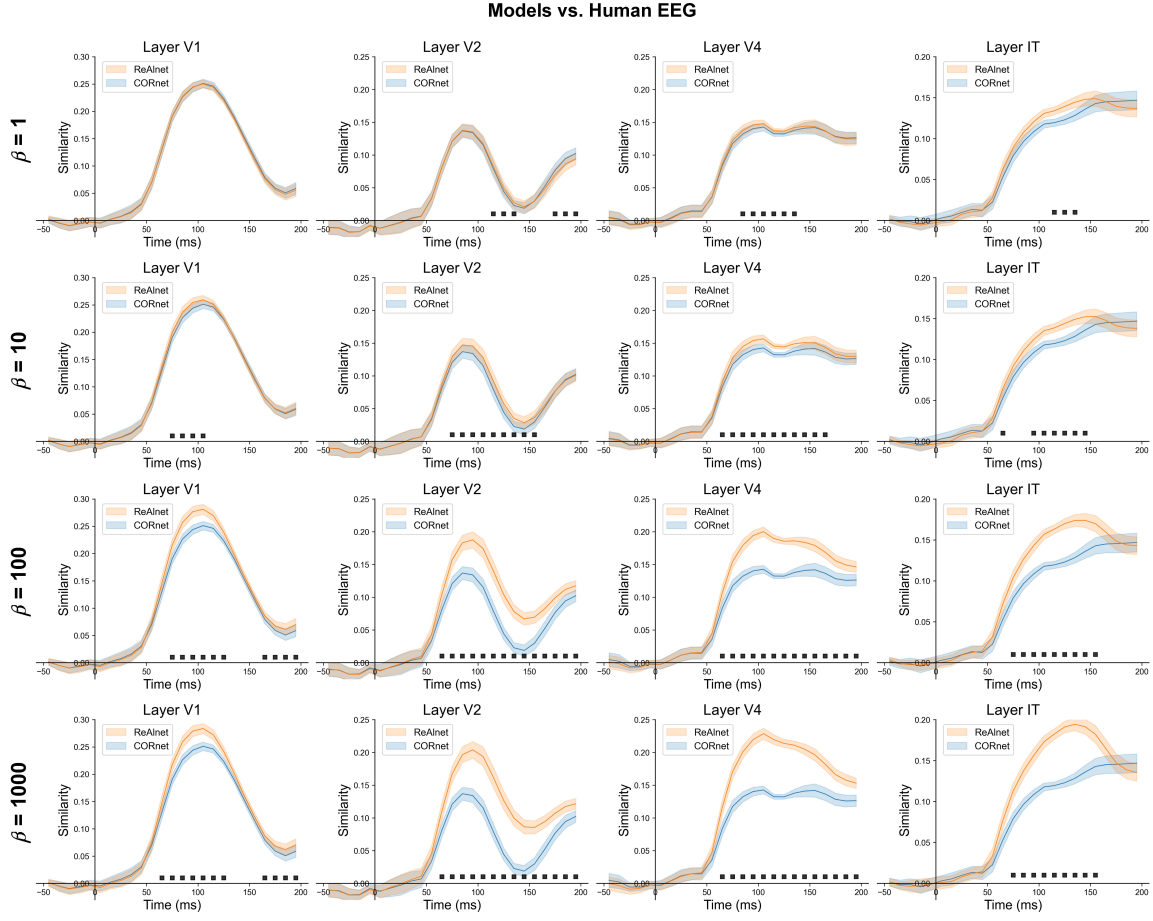


Figure S7: Representational similarity time courses between human EEG and different ReAlnets for different layers respectively. Black square dots at the bottom indicate significant timepoints ($p < .05$). Shaded area reflects \pm SEM.

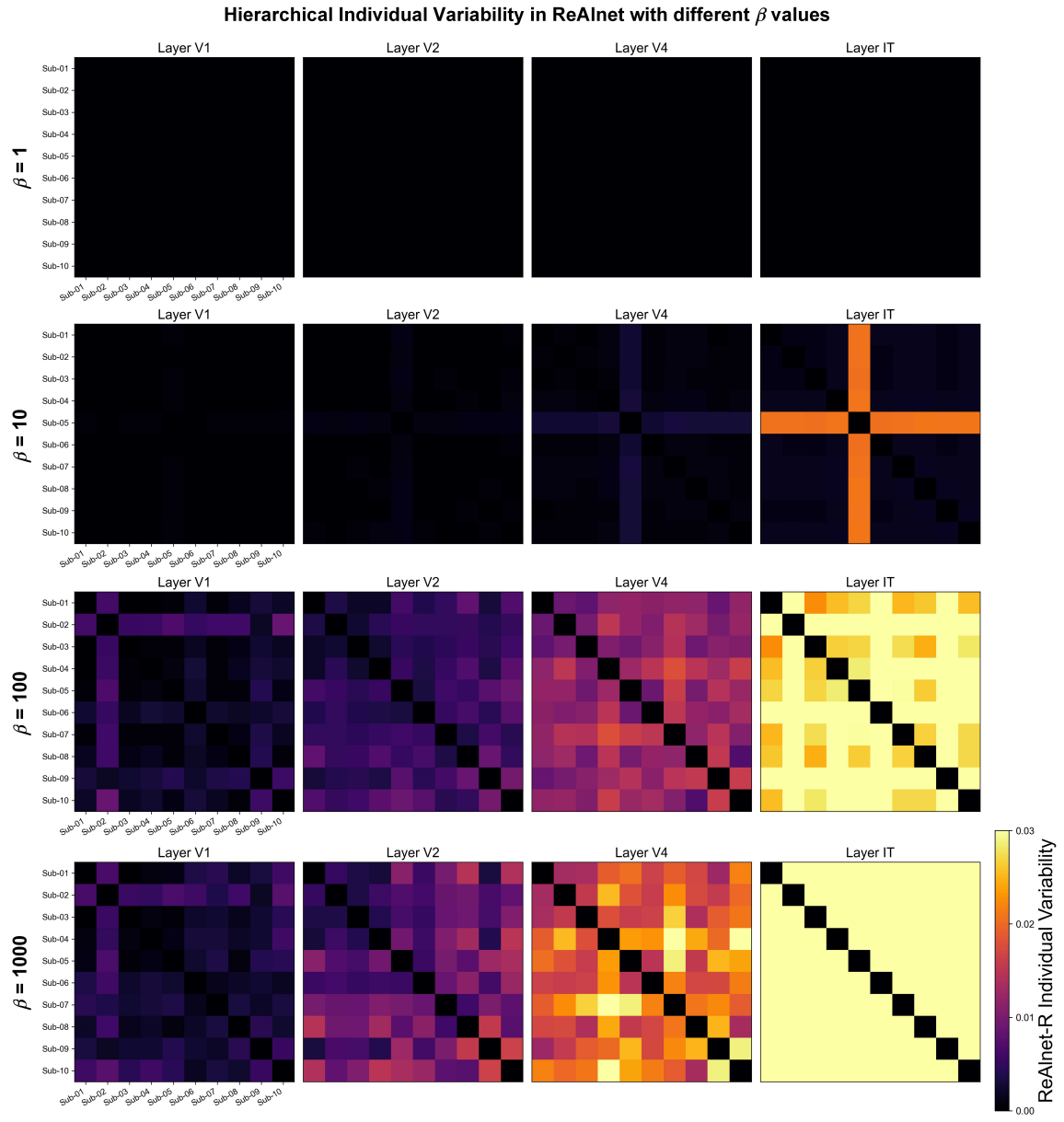


Figure S8: Individual variability matrices of four visual layers of different ReAlnets.

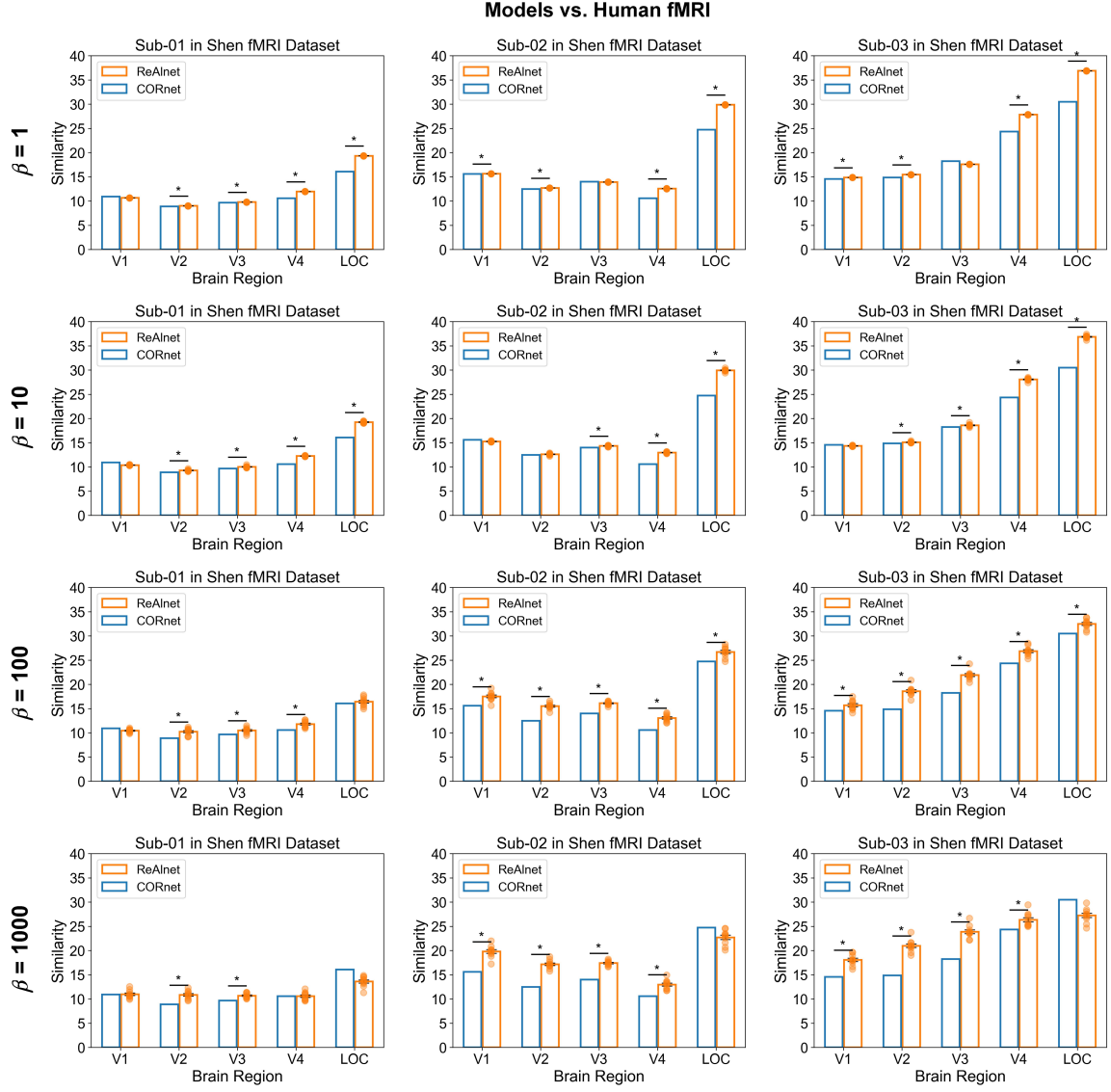


Figure S9: Representational similarity between three subjects' fMRI activity of five different brain regions when they viewed natural images and different ReAlnets respectively. Asterisks indicate significantly higher similarity of ReAlnet than that of CORnet ($p < .05$).

Models vs. Human Behavior

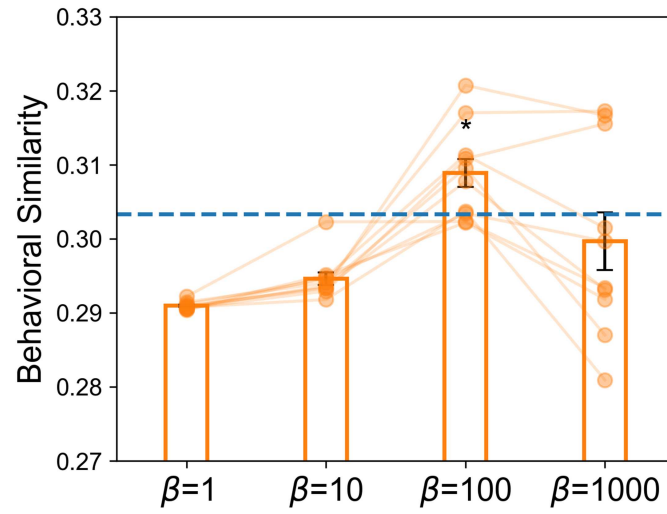


Figure S10: Similarity between human behavior and different ReAlnets based on the Brain-Score platform. Blue dotted line indicates the behavior similarity of CORnet. Each circle dot indicates an individual ReAlnet. Asterisks indicate significantly higher similarity of ReAlnet than that of CORnet ($p < .05$).